ACS NANO

www.acsnano.org

ARTICLE

A Fully Self-Powered Vibration Monitoring System Driven by Dual-Mode Triboelectric Nanogenerators

Shaoxin Li, Di Liu, Zhihao Zhao, Linglin Zhou, Xing Yin, Xinyuan Li, Yikui Gao, Chuguo Zhang, Qing Zhang, Jie Wang,* and Zhong Lin Wang*

Cite This: https://dx.doi.org/10.1021/acsnano.9b10142 Read Online

ABSTRACT: **Vibration sensor is very necessary for monitoring the structural health of constructions. However, it is still a major challenge to meet simultaneously real-time monitoring, continuous assessment, and early incident warning in a simple device without a complicated power and analysis system. Here, we report a self-powered vibration sensor system to achieve real-time and continuous detection of the vibration characteristics from a dual-mode triboelectric nanogenerator (AC/DC-TENG), which can produce either alternating current (AC) or direct current (DC) within different operation zones. Within the vibration-safe region, the AC/DC-TENG with AC output not only can continuously assess the vibration characteristics but also can power the signal transmission. More importantly, once the vibration amplitude crosses the danger threshold, the AC converts immediately to DC, meanwhile triggering the alarm system directly to accurately predict the danger of construction. Our self-powered vibration sensor system can serve as a facile tool for accurately monitoring the structural health of constructions.**

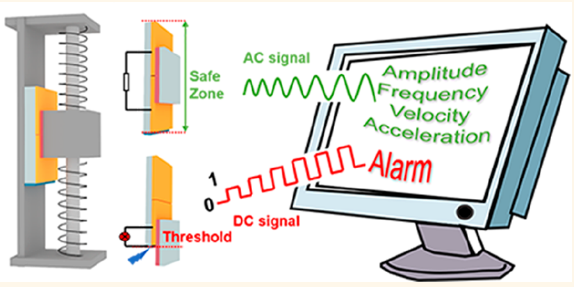

KEYWORDS: *self-powered system, vibration threshold monitoring, triboelectric nanogenerator, real-time alarm system, dual-model structure*

As the operation time increases, the civil construction performance, caused by overstressing, material aging, lack of predictive maintenance, *etc.*, will degrade progressively and result in potential safety hazard problems. The unexpected failures of architectural structure inevitably lead to tremendous life damage and property losses. In order to keep the construction in good operation condition, except for the appropriate structural design, fine construction norms, and periodic maintenance, its real-time operation condition monitoring is also a necessary preventive measure.[1,2] A fiber optic sensor, which is a vibration sensor based on measuring electrical signal changes caused by light signal variations, has been successfully applied for long-term structural health monitoring of large-scale bridges, owing to their attractive characteristics of distributed sensing and simple structure.[3] However, the measurement result errors caused by slight source fluctuation and high-cost fiber materials limit the wide application of fiber optical sensors. Therefore, the direct transition of fundamental vibration parameters (*e.g.*, acceleration, velocity, displacement) into electrical signals is an intuitive feedback method about the assessment of construction movement in different environments.[4] Thus, vibration-monitoring sensors, which could detect vibrations by unmanned aerial vehicles, cameras, piezoelectric sensors, smartphones, and mobile sensors, have been developed based on vibration-based condition measurement.[5] These smart sensors have the advantages of high accuracy, high sensitivity, and capabilities of storing and managing high volumes of data combined with computer technology. Nevertheless, these sensors need batteries or other energy storage devices to operate, resulting in limited lifespan, high recovery and replacement costs, and intractable pollution problems.

A new category of self-powered sensors, which can rationally harvest the ambient energy and operate well without a battery, is highly desirable in recent years.[6−17] Self-powered vibration-monitoring sensors based on a triboelectric nanogenerator (TENG) have received wide attention, because its output

Received: December 26, 2019
Accepted: February 10, 2020
Published: February 10, 2020

electrical signal characteristics are closely related to the parameters of input mechanical behaviors (amplitude, frequency, *etc.*).[18−20] For example, a contact-mode freestanding alternative current TENG (AC-TENG) was reported to quantitatively measure the vibration amplitude through monitoring the voltage or current outputs of AC signals.[21,22] What is more, a sliding-mode freestanding AC-TENG was designed as a vibration accelerator sensor.[23] Although these devices based on an AC-TENG can realize self-powered sensing, they still need external electric energy to drive auxiliary instruments (data acquisition card, electrometer, voltmeter, amperometer, and computer) to collect and then analyze the electrical signals to judge the actual vibration parameters.

In order to realize fully self-powered amplitude threshold monitoring while retaining the accuracy of a vibration-monitor sensor, we designed a dual-mode triboelectric nanogenerator (AC/DC-TENG), which is able to produce either an AC or DC signal within different operation zones. This integrated dual-mode TENG (AC/DC-TENG) vibration monitoring sensor provides a multifunctional response under different vibration amplitudes: within the safe vibration amplitude region, only AC signals are produced by the AC-TENG, which can be stored in an energy storage device for powering signal transmission to a remote monitoring system;[24] over the safe threshold, the DC signals occur and accurately drive a real-time alarm. Apart from the vibration amplitude, other vibration parameters (*e.g.*, frequency and acceleration) can also be sensed by the AC-TENG. In a word, the AC/DC-TENG fully self-powered the vibration amplitude threshold monitoring system and can achieve real-time monitoring of the secure state of vibration without external power or software.

RESULTS AND DISCUSSION

Structure of the AC/DC-TENG. With the rapid progress of material science and architectural techniques, modern buildings are developing toward being higher, longer, and lighter and having different shapes. To ensure the structural safety and healthy operation while reducing the maintenance cost and the loss of property and people, establishing a structural health monitoring system that can warn of early possible construction failure is an extremely effective and important safeguard means.[25] Here, we designed an AC/DC-TENG to drive a fully self-powered vibration amplitude threshold monitoring system (Figure 1a) for detecting the working state of construction (taking a bridge as an example). The structure of the AC/DC-TENG is composed of a stator and a slider, as shown in Figure 1b. The stator is made of two friction electrodes (FEs), a charge collecting electrode (CCE), and an acrylic layer as supporting substrate (SS). Two FEs of equal size (20 mm × 20 mm) are pasted side by side on the acrylic substrate, with a gap of 0.5 mm, and a CCE is placed on the bottom edge of the acrylic substrate. The slider (20 mm × 20 mm) is attached to a fluorinated ethylene propylene (FEP) film as a triboelectric layer (TEL). When the slider slides in a reciprocating manner between two FEs but not over the edge of the acrylic substrate, namely, in the safe zone, the AC signal is generated and flows between the two FEs due to the effects of triboelectrification and electrostatic induction (Figure 1b),[26] and a vibration behavior parameter is obtained through the computer. This working mode belongs to the AC-TENG, and its detailed process is shown in Figure S1a.[27] When a part of the slider moves off the edge of the acrylic substrate, namely, in the danger zone, air breakdown will occur between the CCE and TEL because of the strong electric field under their tiny gap, resulting in a DC signal in the external circuit and driving the alarm light directly (Figure 1b).[28−30] More importantly, the signal type conversion between AC and DC of the AC/DC-TENG within and exceeding the vibration threshold can be used as 0−1 binary code signals in computer programming to combine with the Internet of Things for signal transmission, owing to the effective operation, easy physical realization, and strong versatility.[31] This working mode belongs to the DC-TENG, and its detailed process is shown in Figure S1b.[29] In a word, two types of electrical signals are produced by the AC/DC-TENG during two different motion zones, respectively, so we can judge the vibration amplitude whether it exceeds the vibration threshold without external equipment (just through monitoring the signal type changes of electrical signals).

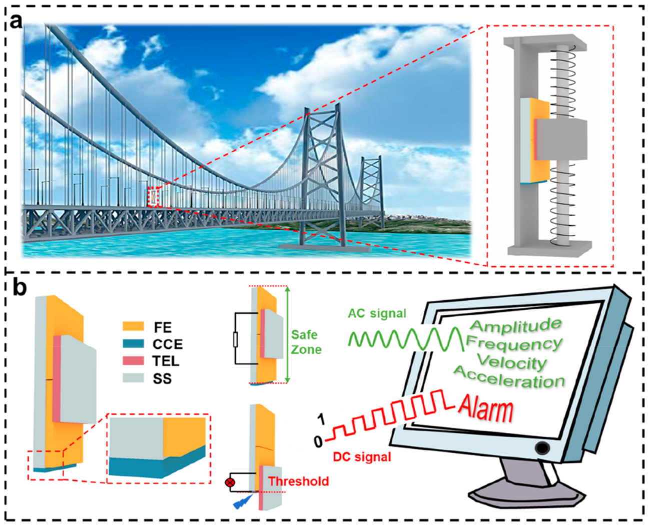

Figure 1. Schematic and experimental structure of a fully self-powered vibration monitoring sensor driven by an AC/DC-TENG. (a) Structure of the AC/DC-TENG. (b) Detailed structure and two different operation zones of the AC/DC-TENG (where FE is the frictional electrode, CCE is the charge-collecting electrode, TEL is the triboelectric layer, and SS is the supporting substrate).

Working Mechanism of the AC/DC-TENG. For a better illustration of the working mechanism, the detailed principle of AC/DC-TENG is illustrated in Figure 2. In the initial state, the slider is fully overlapped with the FE. Due to the contact electrification effect, the FE surface shows positive charges, accompanied by the negative charges on the FEP surface. The working principle of the AC/DC-TENG can be elucidated as two aspects. Under the safe threshold, the single motion cycle of AC/DC-TENG is i → ii → iii → iv → v → i, as shown in Figure 2a. The slider slides in a reciprocating manner between two FEs, resulting in a back-and-forth flow of electrons (*i.e.*, AC) between two FEs by electrostatic induction. The electrical signals of this process correspond to I_{AC1}/U_{AC1} (i → ii → iii) and I_{AC4}/U_{AC4} (iii → iv → v), as shown in Figure 2b and c. If part of the slider moves off the far edge of the FE (v → vi), because of the high electrostatic field between the CCE and the negatively charged FEP surface, the air breakdown occurs in the tiny gap, causing a DC in the external circuit, which was confirmed by our previous research.[29] The DC signals will remain until the whole slider moves off the far edge of the FE (I_{DC1}/U_{DC1}). When the slider moves back (vi → i), a large number of electrons on the FEP surface have been consumed

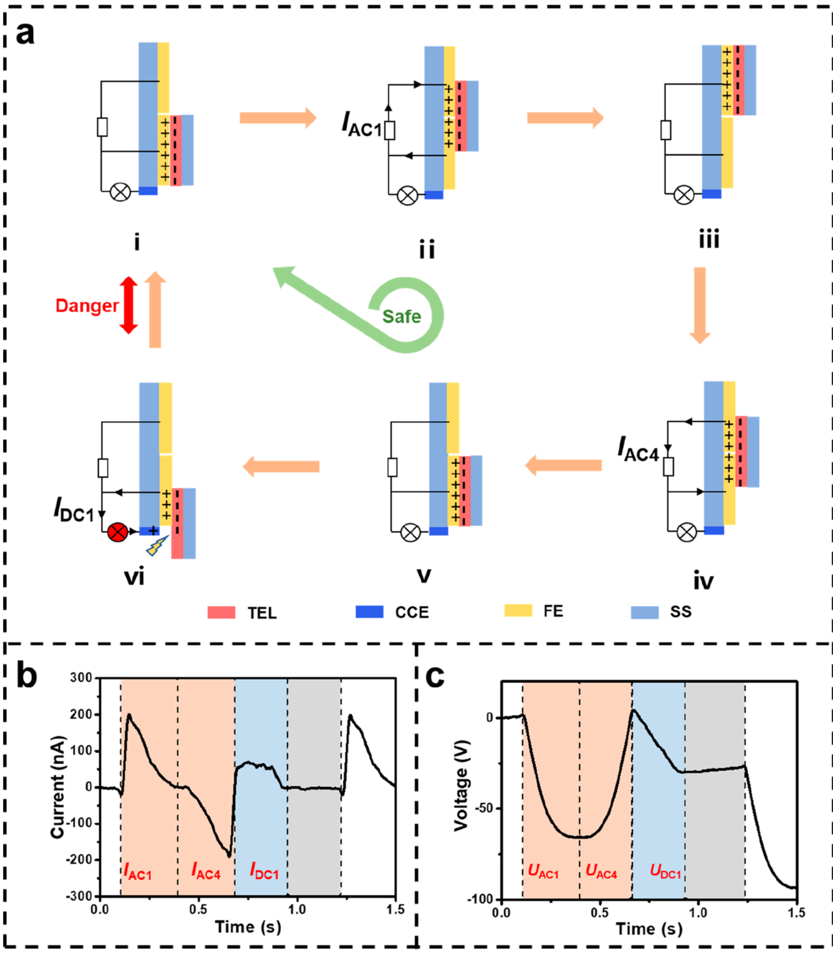

Figure 2. Working mechanism of the AC/DC-TENG. (a) Working process of the AC/DC-TENG. (b) Output current of the AC/DC-TENG with different motion processes. (c) Output voltage of the AC/DC-TENG with different motion processes.

in the last process (v → vi); thus the electric field in the gap is not strong enough to break through the air, resulting in no DC and voltage output (gray region, Figure 2b and c).

To confirm the effect of the CCE, the output performance of the slider moves out of the FE but without the CCE is carried out (Figure S2a). Weak AC signals of this procession are produced between two FEs, as shown in Figure S2b, because this is a simple sliding mode AC-TENG. Compared to just AC signals, adding the CCE to produce DC signals not only can improve the accuracy of amplitude threshold judgment by the switching of different electrical signal types but also can drive a real-time alarm system without external equipment.[29] Therefore, our system can be used as a vibration amplitude threshold detector and achieve fully self-powered amplitude threshold alarming by DC.

Output Performance of the AC/DC-TENG. When the slider vibrates in the safe zone, the output characteristics of V_{AC} (the open-circuit voltage of the AC-TENG) are proportional to the vibration amplitude, as shown in Figure 3a and b. The relationship between V_{AC} and Δx can be explained with the following formula:

$$\Delta V_{AC} = \frac{\Delta Q_{AC}}{C_{AC}} = \frac{\sigma_{AC}\Delta S_{AC}}{C_{AC}} = \frac{\sigma_{AC}W}{C_{AC}}\Delta x \tag{1}$$

where σ_{AC} is the transferred charge density in each vibration within the safe region, C_{AC} is the equivalent capacitance between the two FEs, W is the width of the single FE, and Δx is the vibration amplitude within the safe zone (0 mm ≤ Δx ≤ 20 mm, Figure S3a). For the AC/DC-TENG device, the σ_{AR}, W, and C_{AC} are all constant; thus, the ΔV_{AC} is well linearly proportional to Δx, as shown in Figure 3a and b. Furthermore, we tested more than 10 000 cycles to prove the good stability of the AC/DC-TENG, as shown in Figure S4. When the vibration amplitude is fixed and the vibration velocity changes, as shown in Figure S5, we found that the peak current has a positive correlation with velocity (the detailed formula is in Supplementary Note 1). Meanwhile, we can also measure the vibration frequency and acceleration by monitoring the current output and calculating the differential value of the current, respectively (Figure S6 and Figure S7). Figure 3c shows the charging curve of a capacitor (1.00 μF) charged by the AC-TENG at different vibration amplitudes and frequencies. The charging rate increases with the increase of the vibration amplitude and frequency, and the capacitor can be charged to 3 V within 46.5 s (displacement: 10 mm; frequency: 2 Hz). Figure 3d depicts the charging curves of different capacitors (0.22, 0.47, 1.00, 2.20, 4.70 μF) charged by the AC-TENG at a vibration amplitude of 5 mm and a vibration frequency of 2 Hz, where the 4.70 μF capacitor can be charged to 3 V within 6 min. Storing the AC generated by the AC-TENG in a capacitor can be used to power auxiliary electronic devices for remote signal transmitting.

https://dx.doi.org/10.1021/acsnano.9b10142
ACS Nano XXXX, XXX, XXX−XXX

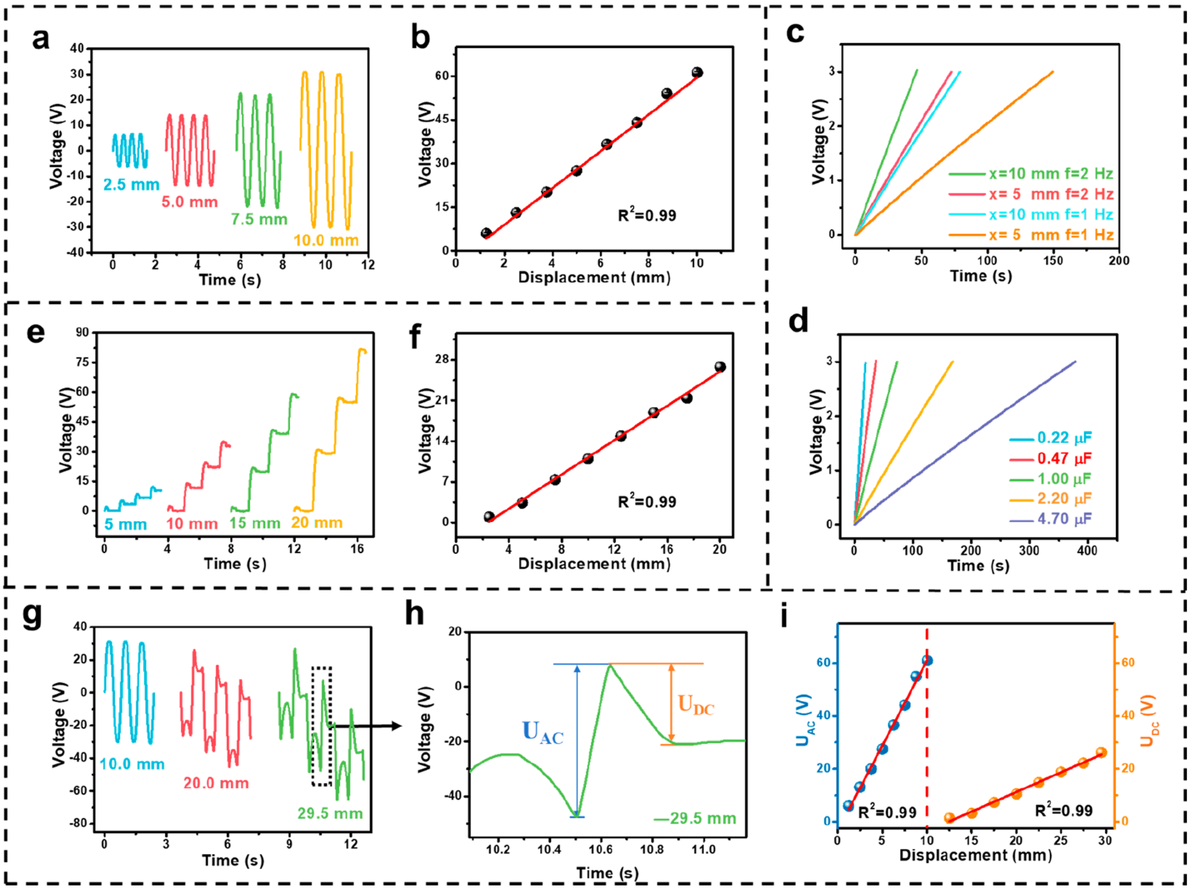

Figure 3. Output performance of the AC/DC-TENG. (a) V_{AC} of the AC/DC-TENG within the safety zone. (b) Relationship between the V_{AC} and Δx. (c) Charging curves of a capacitor (1 μF) charged by the AC/DC-TENG at different vibration amplitudes and frequencies. (d) Charging curves of different capacitors charged by the AC/DC-TENG at a vibration amplitude of 5 mm and a vibration frequency of 2 Hz. (e) V_{DC} of the AC/DC-TENG when the vibration amplitude is over the threshold. (f) Relationship between the V_{DC} and Δy. (g) Output voltage of the AC/DC-TENG at various working stages. (h) Enlarged view of the output voltage of the AC/DC-TENG. (i) Linear relationship between V_{AC} and Δx or V_{DC} and Δy, respectively.

When the slider moves out of the amplitude threshold, namely, in the danger range, the V_{DC} (the potential between the FE and CCE) of the DC-TENG at different vibration amplitudes is shown in Figure 3e. The V_{DC} depends on the amount of charges ionized by air breakdown, and the number of ionizing charges is directly proportional to the swept area (*i.e.*, the sliding out distance of the slider) of the CCE. This result can be explained by the following formula:

$$\Delta V_{DC} = \frac{\Delta Q_{DC}}{C_{DC}} = \frac{\sigma_{DC}\Delta S_{DC}}{C_{DC}} = \frac{\sigma_{DC} W}{C_{DC}}\Delta y \quad (2)$$

where σ_{DC} is the transferred charge density in each vibration amplitude over the amplitude threshold, C_{DC} is the equivalent capacitance between the FE and CCE, W is the width of the single FE, and Δy is the vibration amplitude over the amplitude threshold (0 mm $\leq \Delta y \leq$ 20 mm, Figure S3b). For the AC/DC-TENG device, the σ_{DC}, W, and C_{DC} are all constant; thus, the ΔV_{DC} is well linearly proportional to Δy, as shown in Figure 3e and f. Therefore, the amplitude distance beyond the amplitude threshold can be characterized by the V_{DC}, and Figure S8 is the illustration of DC collected by the CCE when the sliding displacement exceeds the threshold.

Figure 3g shows the voltage signal type changes of AC/DC-TENG at several specific amplitudes in the safe and danger zones, respectively, and Figure 3h is an enlarged view of the voltage signals of the AC/DC-TENG at the vibration amplitude exceeding the amplitude threshold by 19.5 mm. According to the characteristics of the output voltage signals produced by the AC-TENG and DC-TENG, the linear relationship between V_{AC} and Δx or V_{DC} and Δy works well in the safe zone or danger zone, respectively (Figure 3i). From Figure S9, we can see that the AC output is not affected by the DC output when the vibration amplitude is over the threshold. Furthermore, besides measuring the vibration in the vertical direction, the oscillation motion in the horizontal direction also can be monitored by the voltage and current signals of the AC/DC-TENG sensor, and its working mechanical and output performance is as shown in Figure S10 and Figure S11.

Application of the AC/DC-TENG in Monitoring Vibration Motion. The structural health monitoring system is greatly significant for preventing a sudden accident caused by the deteriorated strength and stiffness of construction over time. A traditional AC-TENG in judging vibration amplitude still needs auxiliary equipment to feedback signal (Figure 4a), resulting in a challenge in the real-time effectiveness of vibration-monitoring sensors. Benefiting from the working mechanism and structure design, our proposed AC/DC-TENG sensor can accurately judge amplitude threshold and is a fully self-powered alarm system, which may be ideal as a vibration detector for monitoring the structural health of a

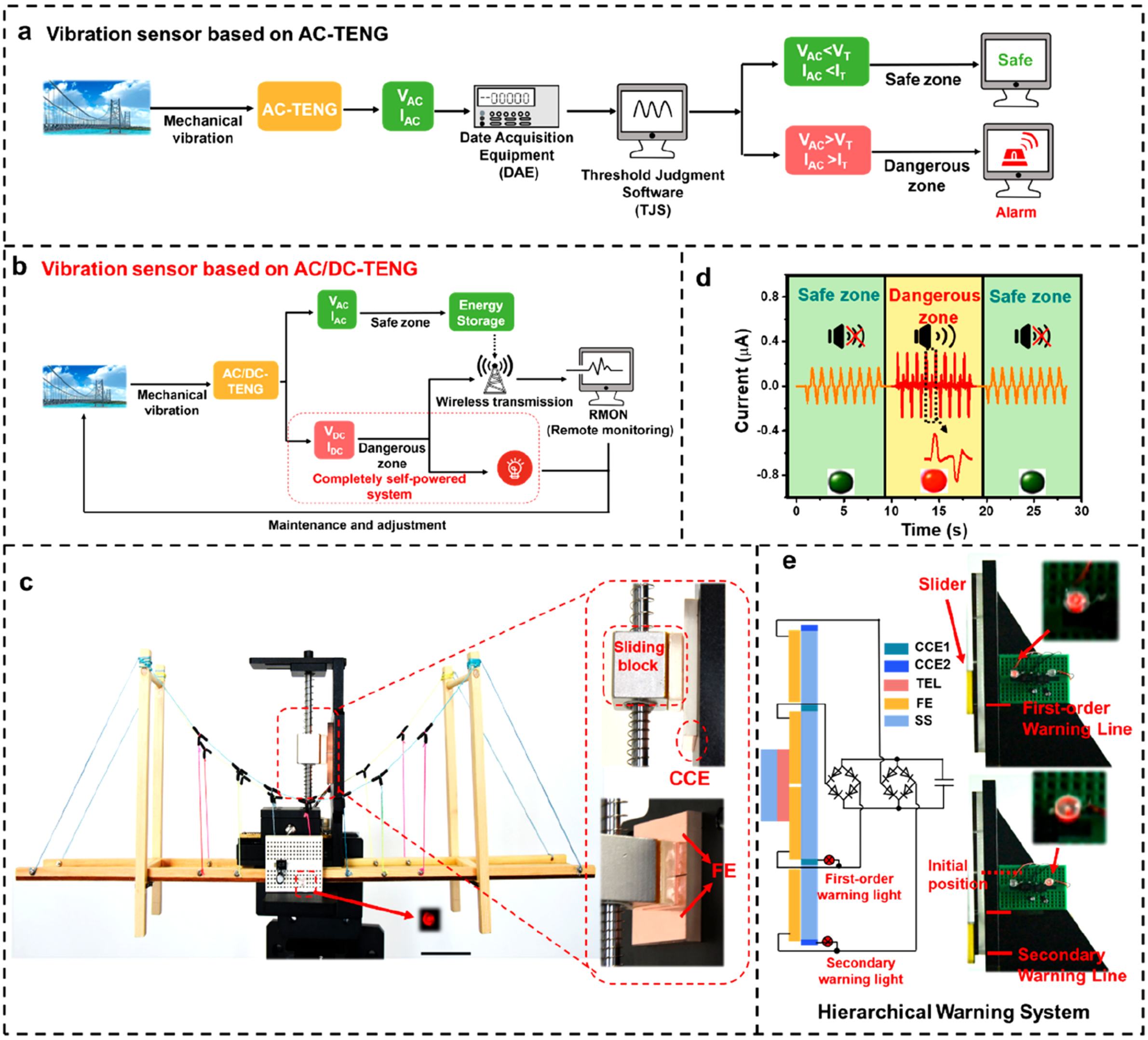

Figure 4. Application of the AC/DC-TENG sensor in monitoring bridge structural health. (a) Operation flow diagram of the self-powered vibration monitoring system based on the AC-TENG sensor. (b) Operation flow diagram of the fully self-powered vibration-monitoring system based on the AC/DC-TENG sensor. (c) Photo of the whole fully self-powered vibration monitoring system on the bridge model. Scale bar: 4 cm. (d) Output current of the AC/DC-TENG at two different vibration amplitude zones. (e) Hierarchical warning system in different working modes.

bridge. Figure 4b shows a flow diagram of the AC/DC-TENG sensor in monitoring vibration behavior of a bridge. If its vibration amplitude is within the safe zone, the AC-TENG part of the AC/DC-TENG sensor converts the mechanical vibration into electrical energy to store in the energy storage unit, and the output power of the AC-TENG is shown in Figure S12. Additionally, the AC output can be improved by increasing the size of the device, selecting materials with excellent triboelectric property, and integrating adjustable circuits.[32−34] When the bridge vibrates so grievously as to move the slider of the AC/DC-TENG sensor over the safe threshold, the DC signals will be generated and drive the red alarm light directly, realizing a real-time alarm. It is worthy to note that this amplitude threshold monitoring and alarm system is fully self-powered without other recognition software. Furthermore, the energy storage device charged by the AC-TENG can power the wireless unit for transmitting data to a remote monitoring location.

In order to simulate the working conditions of the AC/DC-TENG sensor, we integrated the whole fully self-powered system with a hard material bracket (width and height are 8 and 14 cm) on a bridge model, as shown in Figure 4c. When the slider vibrates in the safe zone, the mechanical energy was converted into electrical energy by the AC-TENG for storing in a capacitor. When part of the slider slides out of the threshold, the DC produced by the DC-TENG drives the red LED light in real time, as shown in Video S1. In order to visually display the electrical signals and the corresponding vibration amplitude during the vibration process, the AC/DC-TENG sensor is fixed on motors as a vibration sensor. The shape of the output current during two different motion ranges is shown in Figure 4d. We can see that the sound and red light work in the danger zone from Video S2. Moreover, through further optimizing the structural design, we also achieve a self-powered vibration displacement hierarchical alarming system (Figure 4e), which can achieve first-order alarming and secondary alarming, for quantifying the severity of amplitude exceeding the threshold, as shown in Video S3. This self-powered vibration displacement hierarchical warning method can provide more detailed information about structural

https://dx.doi.org/10.1021/acsnano.9b10142
ACS Nano XXXX, XXX, XXX−XXX

damage for faster judgment and maintenance in civil and building engineering.

CONCLUSION

We have reported the design and fabrication of a dual-mode TENG to achieve a fully self-powered vibration threshold monitoring system, which is integrated with a traditional freestanding AC-TENG and a DC-TENG. Our approach addresses the amplitude threshold self-powered monitoring accuracy and real-time effectiveness issues of a traditional self-powered sensor by detecting the signal type switching of AC and DC signals and using DC output drives an alarm system directly. Furthermore, this system can continuously monitor the vibration amplitude and velocity according to the electrical signal produced by the AC/DC-TENG. With these capabilities, the AC/DC-TENG could provide a convenient and effective avenue for monitoring the structural health of construction.

METHODS

Fabrication of the AC/DC-TENG Sensor. The fabrication process of the AC/DC-TENG is divided into two major steps: (i) the slider consists of three layers; the bottom layer is a piece of acrylic with a thickness of 5 mm as slider substrate, and it is cut into a square with side length of 20 mm by a laser cutter (PLS6.75, Universal Laser Systems). The interlayer is a piece of square foam with the same size as the slider substrate and a thickness of 1 mm as a buffer layer to decrease the hard abrasion between the FEP film and melt electrode. The top layer is a piece of FEP film with the same size as slider substrate and a thickness of 30 μm as a triboelectric layer. (ii) The stator is made of a substrate, two FEs, and a CCE. Similarly, a piece of acrylic with a thickness of 5 mm and size of 20 mm × 40.5 mm was cut by a laser cutter as a stator substrate, and then two FEs of equal size (20 mm × 20 mm) were stuck side by side on the acrylic plate with a small gap of 0.5 mm between them. A piece of CCE with a size of 20 mm × 5 mm was pasted on the side of the acrylic plate along the vertical direction.

Integration of the Fully Self-Powered Vibration Monitoring System and AC/DC-TENG. The fabrication process of this system consists of a fixed rigid support frame, a vibration module, and a circuit manager. The fixed rigid support frame is used to support the stator part of the AC/DC-TENG. The vibration module is made of a fixed rod, two springs, and a stainless-steel cube. The slider was installed on the stainless-steel cube, and the cube was placed in the middle of two springs; then they were all strung on a fixed rod. The circuit manager is made of a rectifier, a capacitor, and a red LED light. The function of the rectifier and capacitor is to store the AC output generated by the AC-TENG. The red LED light connected between the FE and CCE is used as an amplitude threshold alarm light.

Electrical Measurement and Characterization. The vibration process is implemented by a linear motor (TSMV120-1S). A programmable electrometer (Keithley Instruments model 6514) is adopted to measure the short-circuit current, transferred charges, and open-circuit voltage of the AC/DC-TENG. A potentiostat (Bio-Logic VSP-300, France) was used to test the charging curves of capacitors charged by AC-TENG charging.

ASSOCIATED CONTENT

Supporting Information

The Supporting Information is available free of charge at https://pubs.acs.org/doi/10.1021/acsnano.9b10142.

Supporting Note 1 providing the formula of the linear relationship of the peak current and velocity; Figures S1−S12 providing the working mechanism of the AC-TENG and DC-TENG; output performance when the slider exceeds the amplitude threshold but without a CCE; two motion ranges of AC/DC-TENG; stability of the AC/DC-TENG; relationship between current and time of the AC/DC-TENG; relationship of vibration frequency and the output current; linear relationship between dI/dt and vibration acceleration; DC signal of the DC-TENG; AC and DC output of the AC/DC-TENG when the vibration amplitude is over the threshold; working mechanism of the AC/DC-TENG oscillating in the horizontal direction; output performance of the AC/DC-TENG oscillating in the horizontal direction; output power of the AC-TENG (PDF)

Video S1: Fully self-powered vibration monitoring system driven by the AC/DC-TENG (AVI)

Video S2: Audio alarm of the AC/DC-TENG (AVI)

Video S3: Self-powered hierarchical warning system (AVI)

AUTHOR INFORMATION

Corresponding Authors

Jie Wang − *Beijing Institute of Nanoenergy and Nanosystems, Chinese Academy of Sciences, Beijing 100083, People's Republic of China; College of Nanoscience and Technology, University of Chinese Academy of Sciences, Beijing 100049, People's Republic of China; Center on Nanoenergy Research, School of Physical Science and Technology, Guangxi University, Nanning 530004, People's Republic of China;* orcid.org/0000-0003-4470-6171; Email: wangjie@binn.cas.cn

Zhong Lin Wang − *Beijing Institute of Nanoenergy and Nanosystems, Chinese Academy of Sciences, Beijing 100083, People's Republic of China; College of Nanoscience and Technology, University of Chinese Academy of Sciences, Beijing 100049, People's Republic of China; School of Materials Science and Engineering, Georgia Institute of Technology, Atlanta, Georgia 30332, United States;* orcid.org/0000-0002-5530-0380; Email: zhong.wang@mse.gatech.edu

Authors

Shaoxin Li − *Beijing Institute of Nanoenergy and Nanosystems, Chinese Academy of Sciences, Beijing 100083, People's Republic of China; College of Nanoscience and Technology, University of Chinese Academy of Sciences, Beijing 100049, People's Republic of China*

Di Liu − *Beijing Institute of Nanoenergy and Nanosystems, Chinese Academy of Sciences, Beijing 100083, People's Republic of China; College of Nanoscience and Technology, University of Chinese Academy of Sciences, Beijing 100049, People's Republic of China*

Zhihao Zhao − *Beijing Institute of Nanoenergy and Nanosystems, Chinese Academy of Sciences, Beijing 100083, People's Republic of China; School of Materials, Sun Yat-sen University, Guangzhou 510275, People's Republic of China*

Linglin Zhou − *Beijing Institute of Nanoenergy and Nanosystems, Chinese Academy of Sciences, Beijing 100083, People's Republic of China; College of Nanoscience and Technology, University of Chinese Academy of Sciences, Beijing 100049, People's Republic of China*

Xing Yin − *Beijing Institute of Nanoenergy and Nanosystems, Chinese Academy of Sciences, Beijing 100083, People's Republic of China; College of Nanoscience and Technology, University of Chinese Academy of Sciences, Beijing 100049, People's Republic of China*

Xinyuan Li − *Beijing Institute of Nanoenergy and Nanosystems, Chinese Academy of Sciences, Beijing 100083, People's Republic of China; College of Nanoscience and Technology, University of Chinese Academy of Sciences, Beijing 100049, People's Republic of China*

https://dx.doi.org/10.1021/acsnano.9b10142
ACS Nano XXXX, XXX, XXX−XXX

Yikui Gao − *Beijing Institute of Nanoenergy and Nanosystems, Chinese Academy of Sciences, Beijing 100083, People's Republic of China; Center on Nanoenergy Research, School of Physical Science and Technology, Guangxi University, Nanning 530004, People's Republic of China*

Chuguo Zhang − *Beijing Institute of Nanoenergy and Nanosystems, Chinese Academy of Sciences, Beijing 100083, People's Republic of China; College of Nanoscience and Technology, University of Chinese Academy of Sciences, Beijing 100049, People's Republic of China*

Qing Zhang − *Beijing Institute of Nanoenergy and Nanosystems, Chinese Academy of Sciences, Beijing 100083, People's Republic of China*

Complete contact information is available at:
https://pubs.acs.org/10.1021/acsnano.9b10142

Author Contributions

□Shaoxin Li, Di Liu, and Zhihao Zhao contributed equally to this work.

Notes

The authors declare no competing financial interest.

ACKNOWLEDGMENTS

This research was supported by the National Key R & D Project from the Minister of Science and Technology (2016YFA0202704), National Natural Science Foundation of China (Grant Nos. 61774016, 51432005, 5151101243, 51561145021), and Beijing Municipal Science & Technology Commission (Z171100000317001, Z171100002017017, Y3993113DF).

REFERENCES

(1) Comanducci, G.; Magalhães, F.; Ubertini, F.; Cunha, Á. On Vibration-Based Damage Detection by Multivariate Statistical Techniques: Application to a Long-Span Arch Bridge. *Struct. Health Monit.* **2016**, *15*, 505−524.

(2) Xu, B.; Song, G.; Masri, S. F. Damage Detection for a Frame Structure Model Using Vibration Displacement Measurement. *Struct. Health Monit.* **2012**, *11*, 281−292.

(3) Ko, J. M.; Ni, Y. Q. Technology Developments in Structural Health Monitoring of Large-Scale Bridges. *Eng. Struct.* **2005**, *27*, 1715−1725.

(4) Yan, Y.; Li, T.; Liu, J.; Wang, W.; Su, Q. Monitoring and Early Warning Method for a Rockfall Along Railways Based on Vibration Signal Characteristics. *Sci. Rep.* **2019**, *9*, 6606.

(5) Sony, S.; Laventure, S.; Sadhu, A. A Literature Review of Next-Generation Smart Sensing Technology in Structural Health Monitoring. *Struct. Control Health Monit.* **2019**, *26*, No. e2321.

(6) Wang, Z. L. Triboelectric Nanogenerators as New Energy Technology and Self-Powered Sensors-Principles, Problems and Perspectives. *Faraday Discuss.* **2014**, *176*, 447−458.

(7) Wang, Z. L.; Chen, J.; Lin, L. Progress in Triboelectric Nanogenerators as a New Energy Technology and Self-Powered Sensors. *Energy Environ. Sci.* **2015**, *8*, 2250−2282.

(8) Fan, F. R.; Tian, Z. Q.; Wang, Z. L. Flexible Triboelectric Generator! *Nano Energy* **2012**, *1*, 328−334.

(9) Wang, S.; Lin, L.; Wang, Z. L. Triboelectric Nanogenerators as Self-Powered Active Sensors. *Nano Energy* **2015**, *11*, 436−462.

(10) Chen, S. W.; Cao, X.; Wang, N.; Ma, L.; Zhu, H. R.; Willander, M.; Jie, Y.; Wang, Z. L. An Ultrathin Flexible Single-Electrode Triboelectric-Nanogenerator for Mechanical Energy Harvesting and Instantaneous Force Sensing. *Adv. Energy Mater.* **2017**, *7*, 1601255.

(11) Yeh, M.-H.; Guo, H.; Lin, L.; Wen, Z.; Li, Z.; Hu, C.; Wang, Z. L. Rolling Friction Enhanced Free-Standing Triboelectric Nanogenerators and Their Applications in Self-Powered Electrochemical Recovery Systems. *Adv. Funct. Mater.* **2016**, *26*, 1054−1062.

(12) Xie, Y.; Wang, S.; Niu, S.; Lin, L.; Jing, Q.; Yang, J.; Wu, Z.; Wang, Z. L. Grating-Structured Freestanding Triboelectric-Layer Nanogenerator for Harvesting Mechanical Energy at 85% Total Conversion Efficiency. *Adv. Mater.* **2014**, *26*, 6599−6607.

(13) Zhou, L.; Liu, D.; Li, S.; Yin, X.; Zhang, C.; Li, X.; Zhang, C.; Zhang, W.; Cao, X.; Wang, J.; Wang, Z. L. Effective Removing of Hexavalent Chromium from Wasted Water by Triboelectric Nanogenerator Driven Self-Powered Electrochemical System-Why Pulsed DC Is Better than Continuous DC? *Nano Energy* **2019**, *64*, 103915.

(14) Wang, J.; Wang, H.; Li, X.; Zi, Y. Self-Powered Electrowetting Optical Switch Driven by a Triboelectric Nanogenerator for Wireless Sensing. *Nano Energy* **2019**, *66*, 104140.

(15) Guo, H.; Pu, X.; Chen, J.; Meng, Y.; Yeh, M.-H.; Liu, G.; Tang, Q.; Chen, B.; Liu, D.; Qi, S.; Wu, C.; Hu, C.; Wang, J.; Wang, Z. L. A Highly Sensitive, Self-Powered Triboelectric Auditory Sensor for Social Robotics and Hearing Aids. *Sci. Robot.* **2018**, *3*, No. eaat2516.

(16) Pu, X.; Guo, H.; Chen, J.; Wang, X.; Xi, Y.; Hu, C.; Wang, Z. L. Eye Motion Triggered Self-Powered Mechnosensational Communication System Using Triboelectric Nanogenerator. *Sci. Adv.* **2017**, *3*, No. e1700694.

(17) Hinchet, R.; Yoon, H.-J.; Ryu, H.; Kim, M.-K.; Choi, E.-K.; Kim, D.-S.; Kim, S.-W. Transcutaneous Ultrasound EnergyHarvesting Using Capacitive Triboelectric Technology. *Science* **2019**, *365*, 491−494.

(18) Xiang, C.; Liu, C.; Hao, C.; Wang, Z.; Che, L.; Zhou, X. A Self-Powered Acceleration Sensor with Flexible Materials Based on Triboelectric Effect. *Nano Energy* **2017**, *31*, 469−477.

(19) Pang, Y. K.; Li, X. H.; Chen, M. X.; Han, C. B.; Zhang, C.; Wang, Z. L. Triboelectric Nanogenerators as a Self-Powered 3D Acceleration Sensor. *ACS Appl. Mater. Interfaces* **2015**, *7*, 19076−19082.

(20) Zhang, H.; Ya, Y.; Su, Y.; Chen, J.; Adams, K.; Lee, S.; Hu, C.; Wang, Z. L. Triboelectric Nanogenerator for Harvesting Vibration Energy in Full Space and as Self-Powered Acceleration Sensor. *Adv. Funct. Mater.* **2014**, *24*, 1401−1407.

(21) Wang, S.; Niu, S.; Yang, J.; Lin, L.; Wang, Z. L. Quantitative Measurements of Vibration Amplitude Using a Contact-Mode Freestanding Triboelectric Nanogenerator. *ACS Nano* **2014**, *8*, 12004−12013.

(22) Yin, X.; Liu, D.; Zhou, L.; Li, X.; Zhang, C.; Cheng, P.; Guo, H.; Song, W.; Wang, J.; Wang, Z. L. Structure and Dimension Effects on the Performance of Layered Triboelectric Nanogenerators in Contact-Separation Mode. *ACS Nano* **2019**, *13*, 698−705.

(23) Yu, H.; He, X.; Ding, W.; Hu, Y.; Yang, D.; Lu, S.; Wu, C.; Zou, H.; Liu, R.; Lu, C.; Wang, Z. L. A Self-Powered Dynamic Displacement Monitoring System Based on Triboelectric Accelerometer. *Adv. Energy Mater.* **2017**, *7*, 1700565.

(24) Zhang, C.; Tang, W.; Han, C.; Fan, F.; Wang, Z. L. Theoretical Comparison, Equivalent Transformation, and Conjunction Operations of Electromagnetic Induction Generator and Triboelectric Nanogenerator for Harvesting Mechanical Energy. *Adv. Mater.* **2014**, *26*, 3580−3591.

(25) Liang, Q.; Yan, X.; Liao, X.; Cao, S.; Lu, S.; Zheng, X.; Zhang, Y. Integrated Active Sensor System for Real Time Vibration Monitoring. *Sci. Rep.* **2015**, *5*, 16063.

(26) Wang, Z. L. On Maxwell's Displacement Current for Energy and Sensors: the Origin of Nanogenerators. *Mater. Today* **2017**, *20*, 74−82.

(27) Wang, S.; Xie, Y.; Niu, S.; Lin, L.; Wang, Z. L. Freestanding Triboelectric-Layer-Based Nanogenerators for Harvesting Energy from a Moving Object or Human Motion in Contact and Non-Contact Modes. *Adv. Mater.* **2014**, *26*, 2818−2824.

(28) Wang, J.; Wu, C.; Dai, Y.; Zhao, Z.; Wang, A.; Zhang, T.; Wang, Z. L. Achieving Ultrahigh Triboelectric Charge Density for Efficient Energy Harvesting. *Nat. Commun.* **2017**, *8*, 88.

(29) Liu, D.; Yin, X.; Guo, H.; Zhou, L.; Li, X.; Zhang, C.; Wang, J.; Wang, Z. L. A Constant Current Triboelectric Nanogenerator Arising from Electrostatic Breakdown. *Sci. Adv.* **2019**, *5*, No. eaav6437.

(30) Luo, J.; Xu, L.; Tang, W.; Jiang, T.; Fan, F. R.; Pang, Y.; Chen, L.; Zhang, Y.; Wang, Z. L. Direct-Current Triboelectric Nanogenerator Realized by Air Breakdown Induced Ionized Air Channel. *Adv. Energy Mater.* **2018**, *8*, 1800889.

(31) Wade, L. Turning History into a Binary Code. *Science* **2015**, *349*, 922.

(32) Liu, W.; Wang, Z.; Wang, G.; Liu, G.; Chen, J.; Pu, X.; Xi, Y.; Wang, X.; Guo, H.; Hu, C.; Wang, Z. L. Integrated Charge Excitation Triboelectric Nanogenerator. *Nat. Commun.* **2019**, *10*, 1246.

(33) Kwak, S. S.; Kim, S. M.; Ryu, H.; Kim, J.; Khan, U.; Yoon, H.-J.; Jeong, Y. H.; Kim, S.-W. Butylated Melamine Formaldehyde as a Durable and Highly Positive Friction Layer for Stable, High Output Triboelectric Nanogenerators. *Energy Environ. Sci.* **2013**, *12*, 3156−3163.

(34) Seol, M.; Kim, S.; Cho, Y.; Byun, K.-E.; Kim, H.; Kim, J.; Kim, S. K.; Kim, S.-W.; Shin, H.-J.; Park, S. Triboelectric Series of 2D Layered Materials. *Adv. Mater.* **2018**, *30*, 1801210.

https://dx.doi.org/10.1021/acsnano.9b10142
ACS Nano XXXX, XXX, XXX−XXX